

Direct Nuclear Reactions in Lithium-Lithium Systems: ${}^7\text{Li}+{}^7\text{Li}$ at $E_{lab} = 2 - 16$ MeV

P. Rosenthal, H. Freiesleben*, B. Gehrman, I. Gotzhein, K. W. Potthast

Institut für Experimentalphysik I, Ruhr-Universität-Bochum,

D-44780 Bochum, Germany

and

B. Kamys, Z. Rudy

Institute of Physics, Jagellonian University, PL-30059 Cracow, Poland

* Present address: Institut für Kern- und Teilchenphysik,

Technische Universität Dresden, D-01062 Dresden, Germany

March 24, 2022

Abstract

Angular distributions of ${}^7\text{Li}({}^7\text{Li},t)$, $({}^7\text{Li},\alpha)$ and $({}^7\text{Li},{}^6\text{He})$ reactions were measured for laboratory energies from 2 - 16 MeV. Exact finite range DWBA analyses were performed with the aim to identify contributions of direct processes and to investigate the applicability of DWBA to such few nucleon systems. It turned out that DWBA can be successfully applied to estimate differential and total cross sections of direct transfer processes in ${}^7\text{Li}+{}^7\text{Li}$ interaction. The direct mechanism was found to play a dominant role in most of these reactions but significant contributions of other, strongly energy dependent processes were also established. It is suggested that these processes might be due to isolated resonances superimposed on the background of statistical fluctuations arising from interference of compound nucleus and direct transfer contributions.

Nuclear Reactions: ${}^7\text{Li}+{}^7\text{Li}$ at $2 \leq E_{lab} \leq 16$ MeV; measured angular distributions and excitation functions of p, d, t, α , and ${}^6\text{He}$ -channels; deduced direct mechanism contribution to t, α and ${}^6\text{He}$ -channels by DWBA analysis; reaction mechanism inferred.

PACS: 25.70.-x; 25.70.Hi

1 Introduction

Prominent clusterization of weakly bound lithium nuclei may influence in various ways the mechanism of reactions in which they take part. A high probability of direct cluster-transfer reactions should be a likely consequence of clusterization, indicated by both large spectroscopic amplitudes and small separation energies of the clusters. They might play a dominant role in the system of two interacting lithium nuclei. However, other reaction mechanisms cannot be excluded since the small binding energy of the entrance channel nuclei leads to a compound nucleus with high excitation energy, i.e. with high density of states. Hence, large compound nucleus cross sections might occur. Furthermore, due to the clusterization, states with a specific, simple structure may appear as isolated resonances [1, 2] superimposed on the statistical background of compound nucleus decay [3].

The aim of the present work is twofold. First, to study the contribution of direct reactions in the ${}^7\text{Li}+{}^7\text{Li}$ system and, in turn, to estimate the magnitude of other possible mechanisms. If direct processes were to contribute significantly we have an opportunity to test the quality of DWBA predictions by straightforward comparison with experimental data and, thus, to investigate the applicability of direct reaction theory in the extreme case of a nuclear system consisting of few nucleons. It is *a priori* not obvious whether the standard DWBA method can be used for such a system since this approach explicitly assumes transfer reactions to be only a perturbation to elastic scattering. This condition may be fulfilled for transfer reaction cross sections because they are typically smaller by an order of magnitude than those of elastic scattering. However, each transfer, even that of a single nucleon, modifies the mass of target and projectile in this light nuclear system to an extent which can hardly be considered as perturbation.

The second intriguing aspect of the ${}^7\text{Li}+{}^7\text{Li}$ system is the possibility to test in DWBA calculations various optical model (OM)

potentials which give an equivalent description of elastic and inelastic scattering data. In a recent extensive investigation of elastic and inelastic scattering in the ${}^7\text{Li}+{}^7\text{Li}$ system [4] no potential could be singled out on the basis of the quality with which experimental data were described. One may hope that cross sections of transfer reactions will be more sensitive to optical model potentials used to generate distorted waves for DWBA calculations than elastic or inelastic scattering cross sections.

It seems likely that both alpha particle transfer ${}^7\text{Li}({}^7\text{Li},t){}^{11}\text{B}$ and the triton transfer ${}^7\text{Li}({}^7\text{Li},{}^4\text{He}){}^{10}\text{Be}$ are the best candidates for direct - transfer reactions due to the very small separation energy of ${}^7\text{Li} \rightarrow {}^4\text{He} + t$. These transfers, however, significantly change the mass of target and projectile during the collision (40 - 60%). Thus, as pointed out above, the applicability of a perturbation theory must be questioned. In this respect, nucleon transfer reactions, namely proton transfer ${}^7\text{Li}({}^7\text{Li},{}^6\text{He}){}^8\text{Be}$ and neutron transfer ${}^7\text{Li}({}^7\text{Li},{}^6\text{Li}){}^8\text{Li}$, are considered most adequate. Unfortunately, the neutron transfer reaction appears to have a negative Q-value and therefore its cross section is very small in the energy range studied here. Thus only alpha particle, triton, and proton transfers were selected for the present investigation. They correspond to triton, alpha particle and ${}^6\text{He}$ exit channels, respectively. The proton and the deuteron exit channels also measured in the present experiment were used to estimate the total fusion cross section and compound nucleus contribution to the reactions under investigation [5].

Studies of ${}^7\text{Li}({}^7\text{Li},t)$ and ${}^7\text{Li}({}^7\text{Li},{}^4\text{He})$ reactions are reported in the literature mainly for low energies ($E_{lab} = 2 - 6$ MeV) [6, 7, 8] with exception of the $({}^7\text{Li},{}^4\text{He})$ reaction for which a forward angle excitation function was measured in the range of $E_{lab} = 2 - 21$ MeV [9]. The ${}^7\text{Li}({}^7\text{Li},{}^4\text{He}){}^{10}\text{Be}$ reaction was also studied at 26 and 30 MeV with the aim to look for resonant states of ${}^{10}\text{Be}$ [10], while the ${}^7\text{Li}({}^7\text{Li},{}^{11}\text{B})t$ reaction was investigated at 79.6 MeV as part of a

study of reactions leading to multi - neutron final states [11]. All these investigations were not concerned with the questions asked here.

The ${}^7\text{Li}({}^7\text{Li}, {}^6\text{He})$ reaction was reported in the literature at very low energies ($E_{lab} = 3$ MeV [12], $E_{lab} = 3-3.8$ MeV [13]) where only spectra at small reaction angles were measured, and at energies above our energy range (Bochkarev et al. [14], $E_{lab} = 22$ MeV). Angular distributions of transitions to the ground and the first excited state of ${}^8\text{Be}$ were found in the latter experiment to show pronounced oscillations and to be rather steep. The authors suggested a direct reaction mechanism since DWBA calculations agreed reasonably well with the experimental data. Moreover, estimation of the compound nucleus contribution made by means of the Hauser-Feshbach model indicated [14] that the compound nucleus mechanism is responsible for only a small part (approximately 10%) of the experimental cross section. Thus the ${}^7\text{Li}({}^7\text{Li}, {}^6\text{He}){}^8\text{Be}$ reaction may be used to study the applicability of the DWBA formalism for this few - nucleon system and for testing various OM potentials in the ${}^7\text{Li}+{}^7\text{Li}$ system.

In the present work angular distributions of light ejectiles (tritons and ${}^4\text{He}$) are measured in the energy range from $E_{lab} = 2 - 16$ MeV while those for ${}^6\text{He}$ are restricted to 8 - 16 MeV. The experimental procedure and results are given in the next chapter. The analysis of the data in the frame of the DWBA formalism is presented in the third chapter while a summary with conclusions is provided in the last one.

2 Experimental procedure

The experiments were carried out at the 4 MV Dynamitron Tandem accelerator at the Ruhr-Universität Bochum. ${}^7\text{Li}$ -beams were produced with a deflection sputter source; for these experiments the beam currents (max. $2.5 \mu\text{A}$ Li^- ions) were limited to 30 nA up to 100 nA (electric) in order not to destroy the targets and

backings. The beam was focused onto the targets via two collimators ($\varnothing = 1.5$ mm) 40 and 60 cm upstream of the target. Targets of metallic lithium in natural isotopic abundance (92.5% ${}^7\text{Li}$, 7.5% ${}^6\text{Li}$) were prepared by evaporation onto different backing materials adapted to each experimental setup.

The standard technique to identify charged particles in low energy nuclear reactions is the ΔE - E -discrimination. This technique was employed with triple telescopes of surface barrier detectors in order to cover the broad dynamical range of the p, d, t, α and ${}^6\text{He}$ exit channels in one measurement. These exit channels were investigated in an energy range from $E_{lab} = 2 - 16$ MeV in steps of 0.5 MeV by measuring the differential cross sections from $\theta_{lab} = 0^\circ - 80^\circ$. Some typical spectra are depicted in Fig. 1.

Due to the identity of projectile and target angular distributions are symmetrical with respect to 90° in the center - of - mass system. Hence, it is sufficient to measure up to 80° in the laboratory system in order to obtain the whole angular distribution.

To determine absolute cross sections for these exit channels three separate experimental setups were utilized:

1. With the first differential cross sections were measured from $\theta_{lab} = 10^\circ - 80^\circ$ in steps of 10° . These measurements were carried out with two triple telescopes. The first telescope with an aperture of 0.311 msr and total energy resolution of 280 keV covered the forward angles from $\theta_{lab} = 10^\circ$ up to 40° . The second telescope (aperture: 0.179 msr; total energy resolution: 240 keV) was used to cover the more backward angles from $\theta_{lab} = 50^\circ$ up to 80° . In front of each telescope aluminium foils were positioned to absorb ${}^7\text{Li}$ ions elastically scattered from the Ni-backing. A thickness from 30 up to $55 \mu\text{m}$ was sufficient depending on beam energy and laboratory angle of the telescopes was sufficient. For this setup transmission targets were used consisting of metallic ${}^7\text{Li}$ with an area density of $55 \mu\text{g} / \text{cm}^2$ evaporated onto a Ni-backing with an

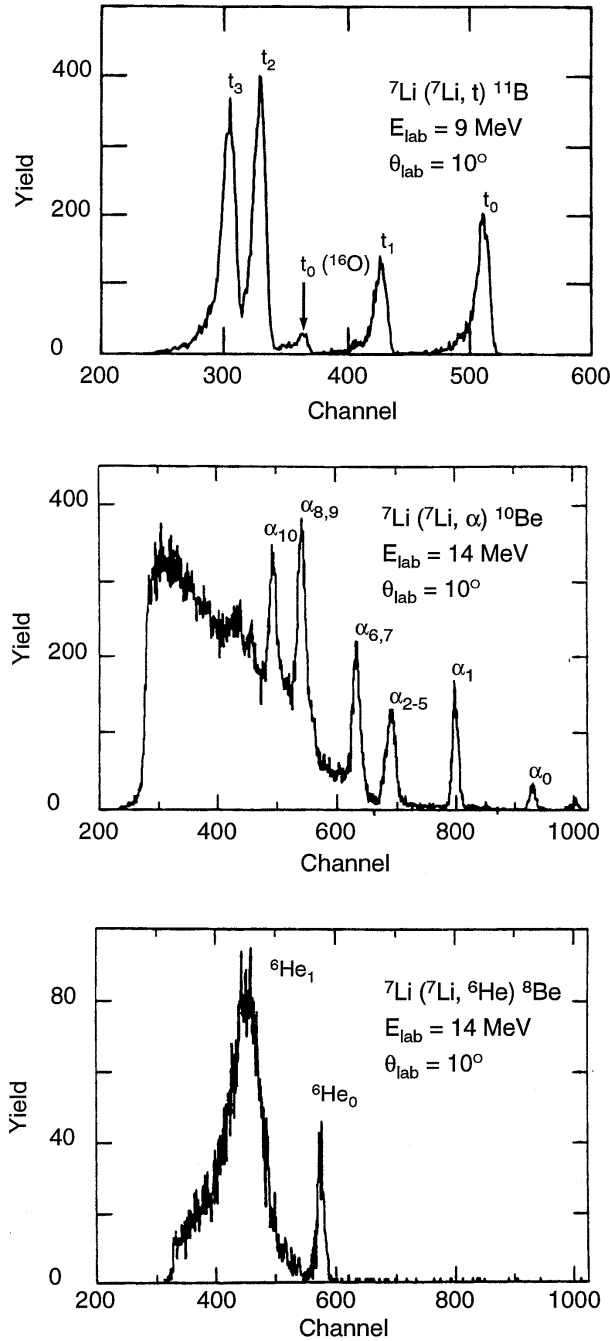


Figure 1: Experimental spectra of tritons ($\theta_{lab} = 30^\circ$, $E_{lab}=9$ MeV), α -particles ($\theta_{lab} = 10^\circ$, $E_{lab}=8$ MeV) and ${}^6\text{He}$ ejectiles ($\theta_{lab} = 10^\circ$, $E_{lab}=16$ MeV)

area density of $90 \mu\text{g} / \text{cm}^2$.

2. The differential cross section of the ${}^7\text{Li}({}^7\text{Li}, \alpha_{0,1}){}^{10}\text{Be}$ reaction at 0° and 5° was measured separately with a special target. It consisted of $55 \mu\text{g} / \text{cm}^2$ metallic ${}^7\text{Li}$ evaporated onto Ni-foils; their thickness of $5.0 \mu\text{m}$ up to $35.4 \mu\text{m}$, depending on beam energy, sufficed to fully stop the ${}^7\text{Li}$ -beam, rendering possible measurements at 0° . One triple telescope with an aperture of 0.314 msr was utilized. Both measurements were carried out independently on absolute scale. The purpose of this second experiment was twofold. First, to extend the angular distributions to 0° , a region which is very sensitive to transfers with orbital angular momentum of $l=0$. Second, to verify the experimental data of Wyborny and Carlson [9] who found very prominent structures in the 0° - excitation function (cf. Fig. 4).

3. For either setup the target thickness was determined via Rutherford scattering of ${}^{58}\text{Ni}^{4+}$ off ${}^7\text{Li}$ in a well defined geometry. Experimental details of target preparation and thickness determination may be found elsewhere [15].

It can be inferred from Fig. 1 that cross sections for triton exit channels are readily determinable for transitions to the ground state and the first three excited states in ${}^{11}\text{B}$. In case of the α -particle exit channel only transitions to the ground and first excited state were evaluated, and for the ${}^6\text{He}$ -exit channel only the ground state transition was selected for the analysis because the higher lying excited states in either case are residing on a continuous background of three particle decays, namely ${}^{14}\text{C}^* \rightarrow {}^9\text{Be} + n + \alpha$ and ${}^{14}\text{C}^* \rightarrow \alpha + {}^{10}\text{Be} \rightarrow {}^6\text{He} + \alpha$, respectively, the shape of which is unknown, rendering rather difficult a reliable evaluation. In Fig. 2 we present an overview of angular distributions for the three ground state transitions investigated. They are represented by a least square fit of a Legendre polynomial expansion to the data. For reason of legibility experimental data are only included for the ${}^6\text{He}$ -channel. Experimental uncertainties are of symbol size, if not shown explicitly.

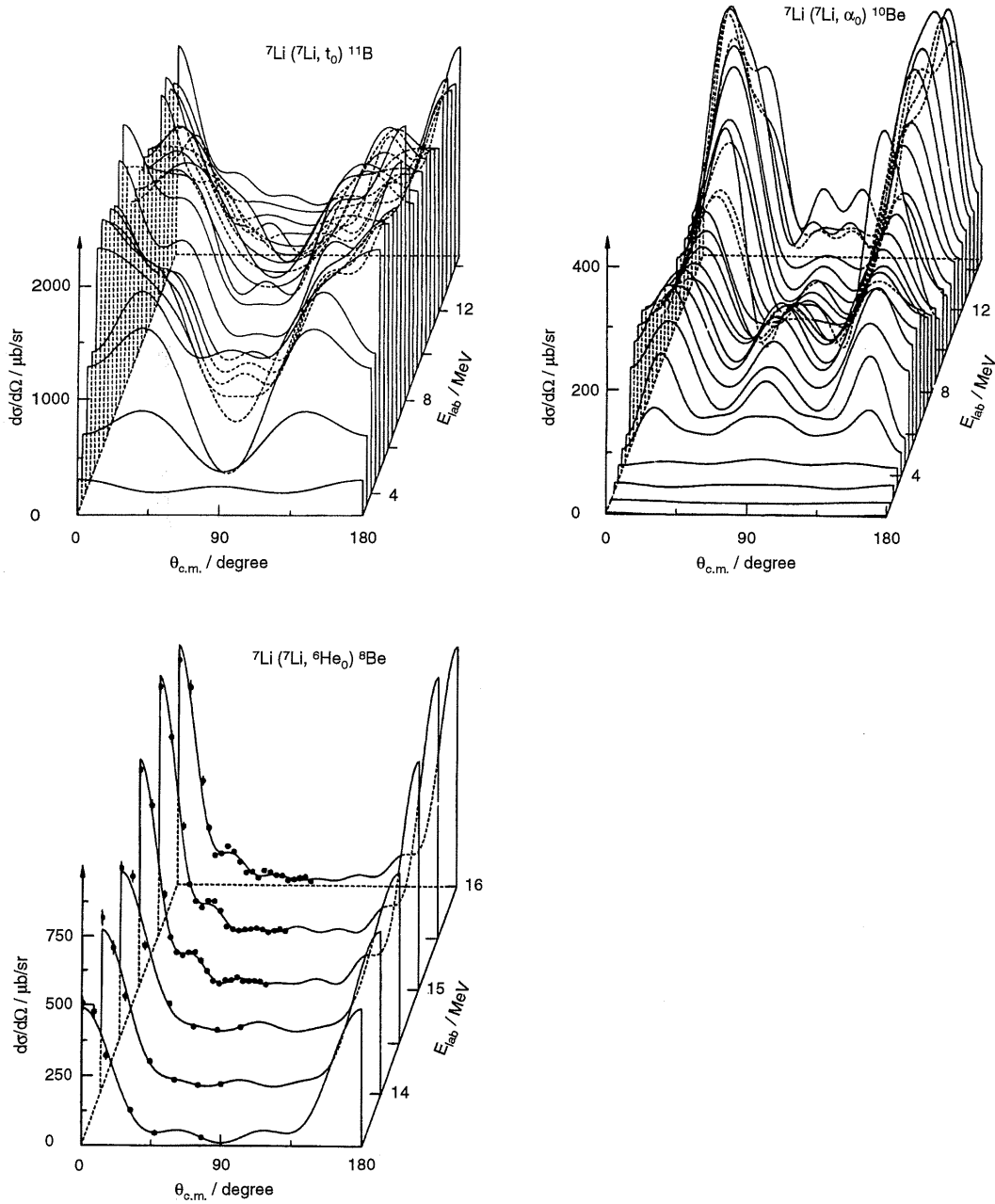


Figure 2: Overview of angular distributions of ground state transitions ${}^7\text{Li}({}^7\text{Li}, t){}^{11}\text{B}$, ${}^7\text{Li}({}^7\text{Li}, \alpha_0){}^{10}\text{Be}$ and ${}^7\text{Li}({}^7\text{Li}, {}^6\text{He}_0){}^8\text{Be}$ represented by result of a least square fit of series of Legendre polynomials to the data. For reason of legibility experimental data are only included for the ${}^6\text{He}$ channel.

Fig. 3 contains the excitation functions of angle integrated cross sections for the triton channel (four lowest states of ${}^{11}\text{B}$), the α -channel (two lowest states of ${}^{10}\text{Be}$) and the ${}^6\text{He}$ -channel

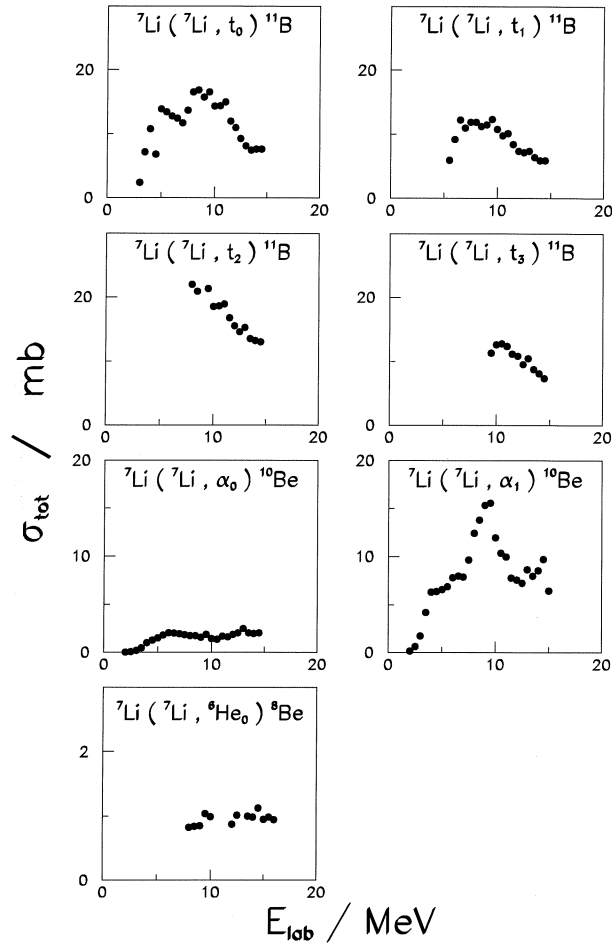


Figure 3: Excitation functions of angle integrated cross sections for ${}^7\text{Li}({}^7\text{Li},t){}^{11}\text{B}$ to the four lowest states of ${}^{11}\text{B}$; (g.s.; $3/2^-$), (2.125 MeV; $1/2^-$), (4.445 MeV; $5/2^-$) and (5.020 MeV; $3/2^-$); excitation functions of angle integrated cross sections for ${}^7\text{Li}({}^7\text{Li},{}^4\text{He}){}^{10}\text{Be}$ to the two lowest states of ${}^{10}\text{Be}$; (g.s.; 0^+) and (3.368 MeV; 2^+) and excitation function of angle integrated cross section for ${}^7\text{Li}({}^7\text{Li},{}^6\text{He}){}^8\text{Be}_{g.s.}$.

(ground state of ${}^8\text{Be}$).

Fig. 4 shows the excitation function for ${}^7\text{Li}({}^7\text{Li},\alpha_1)$ measured at 0° together with the data of Wyborny and Carlson [9]. A very good agreement can be stated.

3 DWBA analysis

The calculations were performed using the exact finite range DWBA computer code Jupiter-5 [16] in both representations (*prior* and *post*) of the transition potentials. In the ideal case of the exact knowledge of transition potentials e.g. from some microscopic model, DWBA calculations should lead to the same result in both representations [17]. Therefore the quality of agreement between results of calculations made within either representations may be taken as indication of both the applicability of the DWBA formalism in its standard form and the proper choice of potentials.

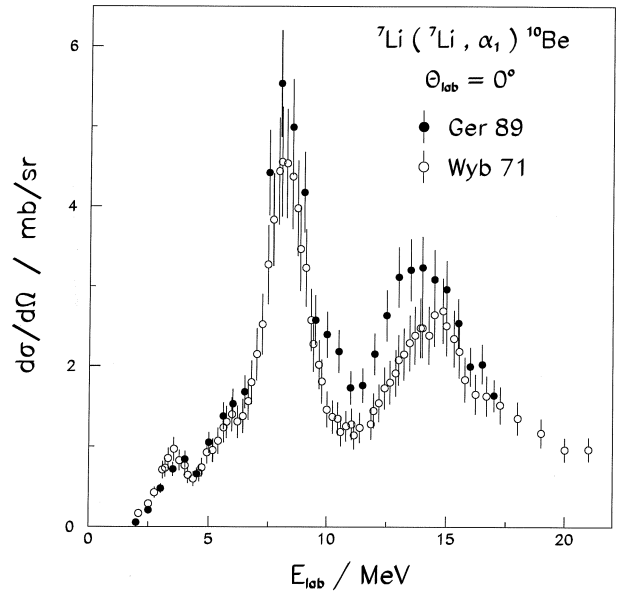


Figure 4: Excitation function for ${}^7\text{Li}({}^7\text{Li},\alpha_1){}^{10}\text{Be}$ measured at $\theta_{lab} = 0^\circ$ (full dots) together with data of Wyborny and Carlson (open dots) [9]

We followed the standard prescription of DWBA for choosing the strong interaction potential responsible for the transfer. This is discussed in the following using the proton transfer reaction ${}^7\text{Li}({}^7\text{Li},{}^6\text{He}){}^8\text{Be}$ as an example. Either the potential which binds the proton to ${}^7\text{Li}$ (*post*) or that which binds the proton to ${}^6\text{He}$ (*prior* representation) was taken as nuclear transition po-

Table 1: Optical model potentials used in the DWBA calculations.

System	Family	U MeV	r_U fm	a_U fm	W MeV	r_W fm	a_W fm	r_C fm	Ref.
${}^7\text{Li}+{}^7\text{Li}$	S-1	3	1.456	1.416	9.8	1.369	0.441	1.25	[4]
	S-2	21	0.802	1.279	13.8	1.354	0.409	1.25	[4]
	S-3	49	0.800	1.036	18.2	1.354	0.387	1.25	[4]
	S-4	69	0.940	0.860	21.2	1.381	0.345	1.25	[4]
	S-5	101	0.965	0.781	23.3	1.397	0.320	1.25	[4]
	S-6	136	0.994	0.721	26.2	1.411	0.296	1.25	[4]
${}^{10}\text{Be}+{}^4\text{He}$	S	136	0.673	0.792	35.6	0.924	0.137	0.795	[20]
${}^{11}\text{B} + t$	V	133	0.923	0.570	19.5	1.090	0.220	0.923	[21]

Real parts of all potentials have the Woods-Saxon form with the following parametrization of radii : $R=r_0*(A_1^{1/3} + A_2^{1/3})$. The imaginary potentials of the "V" families have the volume shape of Woods-Saxon form while those of the "S" families use the surface shape of derivative of Woods-Saxon form.

tential.

Thus it was assumed that perfect cancellation occurs of the so called "indirect transition potentials" i.e. the core-core (${}^7\text{Li}-{}^6\text{He}$) interaction potential is equivalent to either the optical model (OM) potential for the ${}^7\text{Li}-{}^7\text{Li}$ channel (*prior* representation) or the optical model potential for the ${}^6\text{He}-{}^8\text{Be}$ channel (*post* representation). Such an assumption seems to be justified because, in contradistinction to a rather good knowledge of entrance/exit channel optical model potentials, the core-core potential is not known and it is necessary to make assumptions concerning this potential. The best approximation should be an optical model potential for scattering of the core - core nuclear system. However, this potential is usually not known, and moreover, it is not obvious at which energy of the relative motion of the core - core system such potential should be taken. Thus the standard prescription for choosing the nuclear transition potential is to approximate the core - core potential by the optical model potential of either the entrance or the exit channel.

The binding potentials were taken in Woods-Saxon form. Their geometrical parameters were arbitrarily fixed at the following values: the reduced radius $r_0 = 0.97$ fm (for symmetri-

cal parametrization i.e. $R=r_0*(A_{core}^{1/3} + A_{cluster}^{1/3})$ and the diffuseness parameter $a = 0.65$ fm. Such values were successfully used when describing the alpha particle transfer in ${}^{14}\text{N}(d, {}^6\text{Li}){}^{10}\text{B}$ reactions [18]. The depth of the potentials was fitted to reproduce the appropriate binding energy.

The Coulomb "indirect transition potentials" were all taken into account in the present analysis and they were used in the standard form of uniformly charged spheres.

The Jupiter-5 computer code evaluates the reaction amplitudes for one orbital of the cluster in the donor and one orbital in the acceptor nucleus. For some reactions e.g. alpha particle transfers to ${}^{11}\text{B}_{g.s.}$, ${}^{11}\text{B}_{4.45}$ and ${}^{11}\text{B}_{5.02}$ two reaction amplitudes must be calculated because of the two different orbitals of an alpha particle cluster in the boron nucleus. The coherent superposition was performed by means of a separate computer code SQSYM [19] which also took care of the antisymmetrization of amplitudes which is required by the identity of projectile and target.

The introduction of free parameters was avoided by the following procedure: The transition potentials were fixed according to the standard prescription described above.

Parameters of optical model potentials

Table 2: Cluster spectroscopic amplitudes used in the DWBA calculations.

Nucleus	Core	Cluster	n	l	j	C*A	Ref.
${}^7\text{Li}_{g.s.}(3/2^-)$	t	${}^4\text{He}$	1	1	1	1.084	[24, 25]
	${}^4\text{He}$	t	1	1	3/2	1.084	[24, 25]
	${}^6\text{He}$	p	0	1	3/2	-0.831	[22]
${}^8\text{Be}_{g.s.}(0^+)$	${}^7\text{Li}$	p	0	1	3/2	1.287	[22]
${}^{10}\text{Be}_{g.s.}(0^+)$	${}^7\text{Li}$	t	1	1	3/2	0.556	[25]
${}^{10}\text{Be}_{3.37}(2^+)$	${}^7\text{Li}$	t	1	1	1/2	0.568	[25]
			1	1	3/2	0.040	[25]
			0	3	5/2	0.604	[25]
			0	3	7/2	-0.299	[25]
${}^{11}\text{B}_{g.s.}(3/2^-)$	${}^7\text{Li}$	${}^4\text{He}$	2	0	0	-0.509	[27]
			1	2	2	0.629	[27]
${}^{11}\text{B}_{2.13}(1/2^-)$	${}^7\text{Li}$	${}^4\text{He}$	1	2	2	-0.585	[27]
${}^{11}\text{B}_{4.45}(5/2^-)$	${}^7\text{Li}$	${}^4\text{He}$	1	2	2	0.725	[26]
			0	4	4	0.018	[26]
${}^{11}\text{B}_{5.02}(3/2^-)$	${}^7\text{Li}$	${}^4\text{He}$	2	0	0	-0.292	[26]
			1	2	2	-0.322	[26]

"n" corresponds to the number of nodes of the bound state radial wave function (excluding $r=0$ and infinity),

"l" is the orbital angular momentum of relative motion of the cluster and the core,

"j" is the total angular momentum of the orbital,

"C*A" denotes the product of the isospin Clebsch-Gordan coefficient and the spectroscopic amplitude.

were taken from the literature, whenever it was possible i.e. for ${}^7\text{Li}+{}^7\text{Li}$ [4], ${}^{10}\text{Be}+\alpha$ [20] and ${}^{11}\text{B}+t$ [21] systems, or they were approximated by ${}^7\text{Li}+{}^7\text{Li}$ potentials for the inaccessible elastic ${}^8\text{Be}+{}^6\text{He}$ channel. All potential parameters are listed in Table 1. The spectroscopic amplitudes were taken from shell model calculations published in the literature for protons [22], tritons [23, 24], and for α - particles [25, 26, 27]. Their values are given in Table 2. In that sense all calculations of cross sections were performed without any free parameter.

3.1 The proton transfer reaction - ${}^7\text{Li}({}^7\text{Li}, {}^6\text{He}){}^8\text{Be}$

A qualitative inspection of the experimental data suggests the $({}^7\text{Li}, {}^6\text{He})$ reaction to be dominated by a direct reaction mechanism. The differential cross section of this reaction is significantly

smaller (at least two orders of magnitude) than the elastic scattering cross section in the ${}^7\text{Li}+{}^7\text{Li}$ system [4] compared at corresponding scattering angles. Therefore one is allowed to treat the proton transfer reaction $({}^7\text{Li}, {}^6\text{He})$ as a perturbation to the elastic scattering and hence to apply the distorted wave Born approximation. Furthermore, the transfer of one nucleon results in a relatively small rearrangement between the interacting lithium nuclei and may thus, also from this point of view, be considered as a perturbation. These arguments led us to consider the ${}^7\text{Li}({}^7\text{Li}, {}^6\text{He}){}^8\text{Be}$ reaction as the best candidate among the reactions under investigation for testing the applicability of DWBA to such light nuclear system.

Calculations of angular distributions for proton transfer were performed for 8, 10, 12, 14 and 16 MeV laboratory energy for which experimental data were measured in the present

work. Additional calculations were performed at an energy of 22 MeV for the reaction leading to both the ground and the first excited state of ${}^8\text{Be}$ rendering possible a comparison with the experimental data of Bochkarev et al. [14].

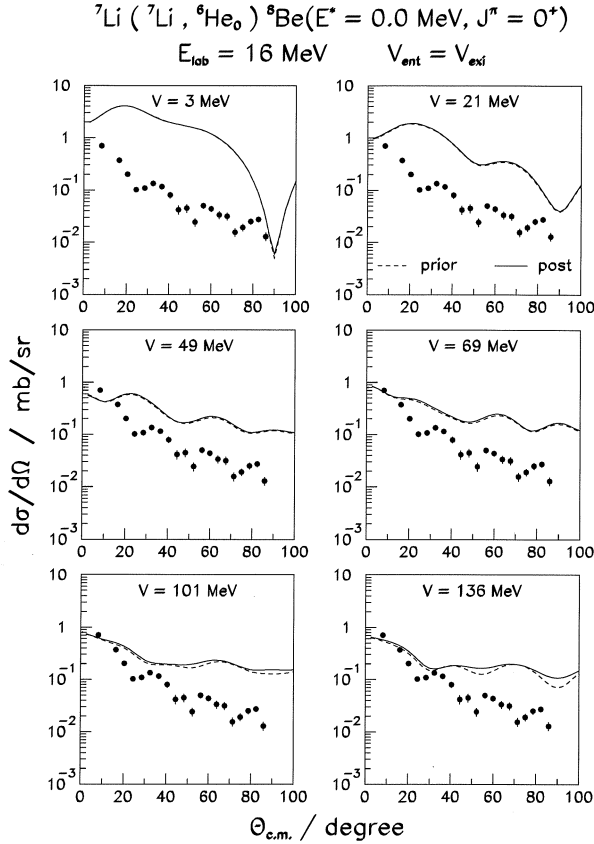


Figure 5: Experimental angular distribution of ${}^7\text{Li}({}^7\text{Li}, {}^6\text{He}){}^8\text{Be}_{g.s.}$ reaction at $E_{lab}=16$ MeV (full dots). Solid and dashed curves represent results of DWBA calculations in *post* and *prior* representation, respectively. Six OM potentials were applied which describe elastic scattering in the ${}^7\text{Li}+{}^7\text{Li}$ system equally well [4]. The "family" of the OM potential parameters is specified by quoting the depth of its real part. The same OM potentials were used in entrance and exit channel.

The quality of reproduction of the experimental data, the similarity of results in *prior* and *post* representations, and the dependence of

the results on the optical model potentials was found to be almost the same for the energies under investigation. Therefore, we present in Figs. 5, 6 and 7 only results for one bombarding energy, i.e., 16 MeV.

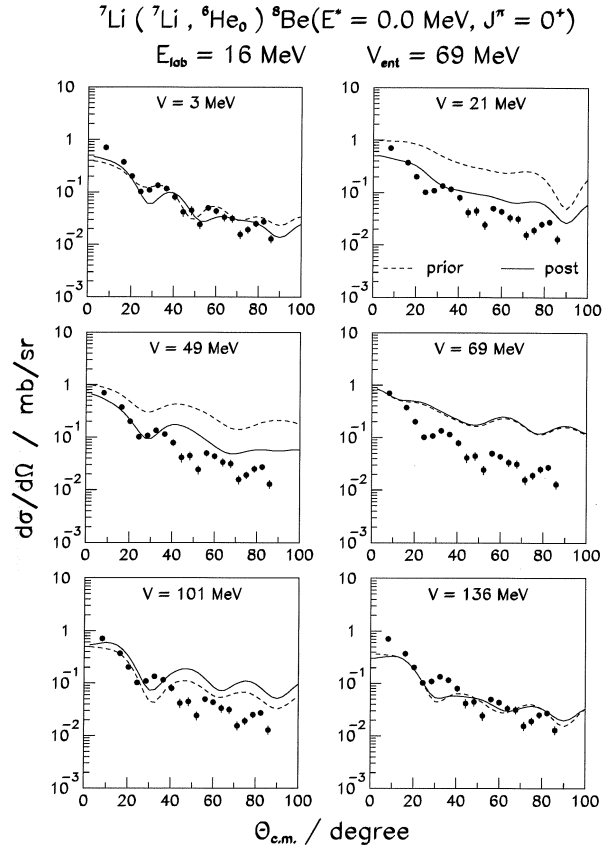


Figure 6: Same as Fig. 5, but the entrance channel OM potential is fixed (family #4, i.e. "69 MeV" of [4]) while all six equivalent potentials of ref. [4] are used for the exit channel.

Identical optical model potentials used for both entrance and exit channel lead to a perfect equivalence of the *prior* and *post* representations. This can be inferred from Fig. 5 where angular distributions evaluated in *prior* (dashed lines) and in *post* representation (full lines) almost coincide for six different "families" of parameters of OM potentials listed in Table 1. Thus we conclude, that DWBA is applicable for this reaction

under the stated conditions.

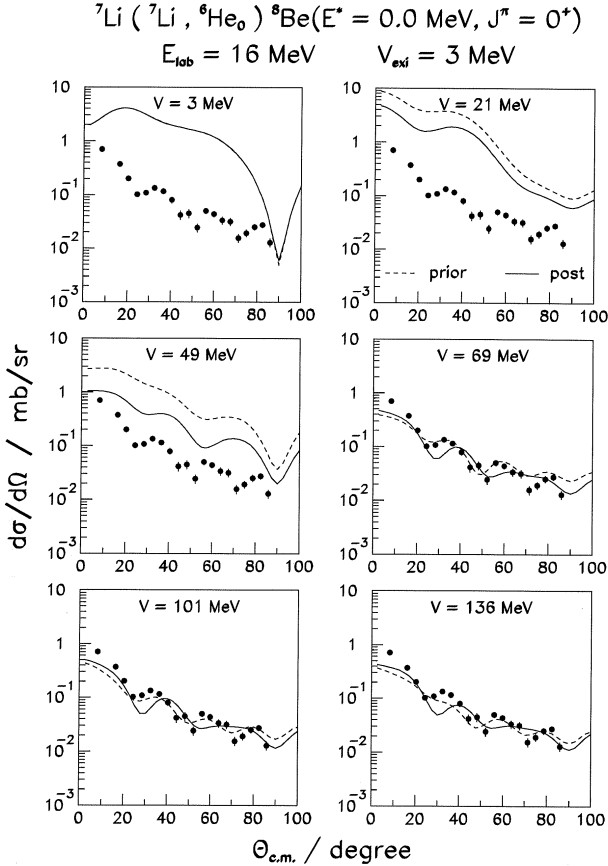


Figure 7: Same as Fig. 5, but the exit channel OM potential is fixed (family #1, i.e. "3 MeV" of [4]) while all six equivalent potentials of ref. [4] are used for the exit channel. Note, that for the most shallow potential in the entrance channel results of calculations in *prior* and *post* representations are almost indistinguishable.

It remains an open question whether the ${}^7\text{Li}({}^7\text{Li}, {}^6\text{He}){}^8\text{Be}$ reaction is realized in nature only via a direct mechanism. It may be answered by comparing the experimental angular distributions with the theoretical ones. It is visible in Fig. 5 that theoretical cross sections surpass the experimental data if the calculations are performed with the shallow optical model potentials. This may hint at the possibility to select some potentials among those which reproduce

equally well the experimental elastic scattering data. However, in order to do so one has to vary the entrance and exit channel OM potentials independently since there is no obvious reason to assume them to be equal. The calculations were thus repeated for all possible pairs of entrance/exit channel potentials listed in Table 1. Figs. 6 and 7 illustrate part of the results obtained.

In Fig. 6 results of calculations are shown obtained with a rather deep potential in the entrance channel ("69 MeV" family) and with various potentials for the exit channel. A reasonable reproduction of the data is possible only for a very shallow potential ("3 MeV" family) in the exit channel. It indicates that in spite of the small difference in mass partition (${}^7\text{Li}+{}^7\text{Li}$ vs. ${}^6\text{He}+{}^8\text{Be}$) completely different optical model potentials seem to be responsible for scattering in these two channels. They may reflect an adiabatic nucleon motion during the ${}^7\text{Li}({}^7\text{Li}, {}^6\text{He}){}^8\text{Be}$ transfer reaction in which the deep entrance channel potential is modified in shape and depth to become the shallow one in the exit channel.

In Fig. 7 the most shallow one from equivalent ${}^7\text{Li}+{}^7\text{Li}$ OM potentials was used in the exit channel ("3 MeV" family), but different potentials were applied in the entrance channel. Again, as in Fig. 5 the shallow potentials in the entrance channel overestimate the cross sections. The potentials deeper than 60 MeV reproduce the experimental angular distributions quite well. Moreover, it can be seen that the agreement of *prior* and *post* representations is better assured by deep entrance channel potentials than by shallow ones (with the exception of identical entrance and exit channel potentials; see above). In summary we conclude that the ${}^7\text{Li}({}^7\text{Li}, {}^6\text{He}){}^8\text{Be}$ reaction favors rather deep OM potentials in the entrance and shallow ones for the exit channel.

In Fig. 8 we present results of the calculations which were performed for several bombarding energies between 8 MeV (lab.) and 22 MeV with this selected pair of OM potentials. The reproduction of the experimental angular distri-

butions may be judged as very good in particular in view of the fact that the calculations were carried out without any free parameters and that cluster spectroscopic factors are known only with some (model dependent) accuracy.

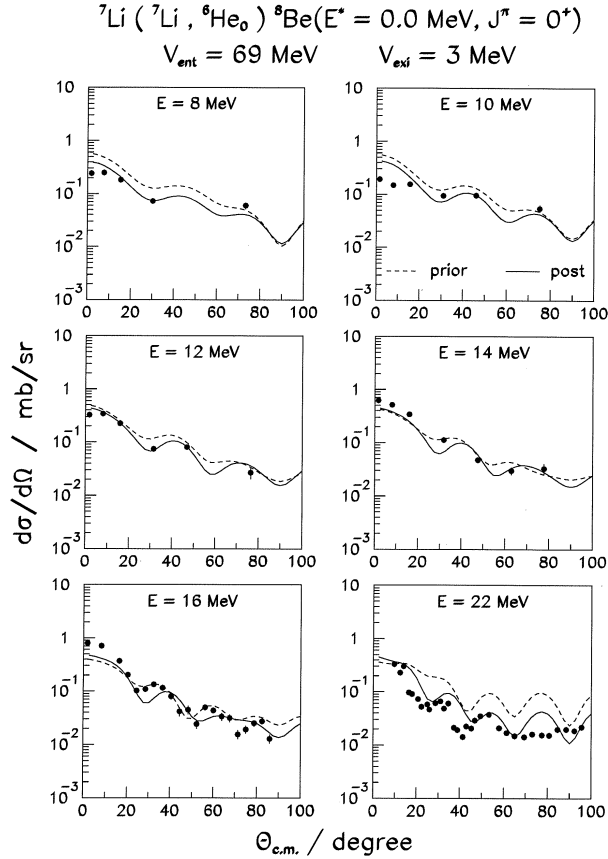


Figure 8: Experimental angular distributions of the ${}^7\text{Li}({}^7\text{Li}, {}^6\text{He}){}^8\text{Be}_{g.s.}$ reaction for several bombarding energies (full dots, present work) together with results of calculations performed with selected pairs of OM potentials: deep potential (family #4, i.e. "69 MeV" of [4]) in the entrance channel and a very shallow one (family #1, i.e. "3 MeV" of [4]) in the exit channel. Full lines correspond to *post*, dashed lines to *prior* representations. The data at $E_{\text{lab}}=22$ MeV were taken from ref. [14].

This good agreement is also seen in the energy dependence of angle integrated cross sec-

tions which are shown in Fig. 9. The dots represent the experimental data of the present work, lines show results of DWBA calculations for *prior* (upper part of the figure) and *post* representation (lower part of the figure)

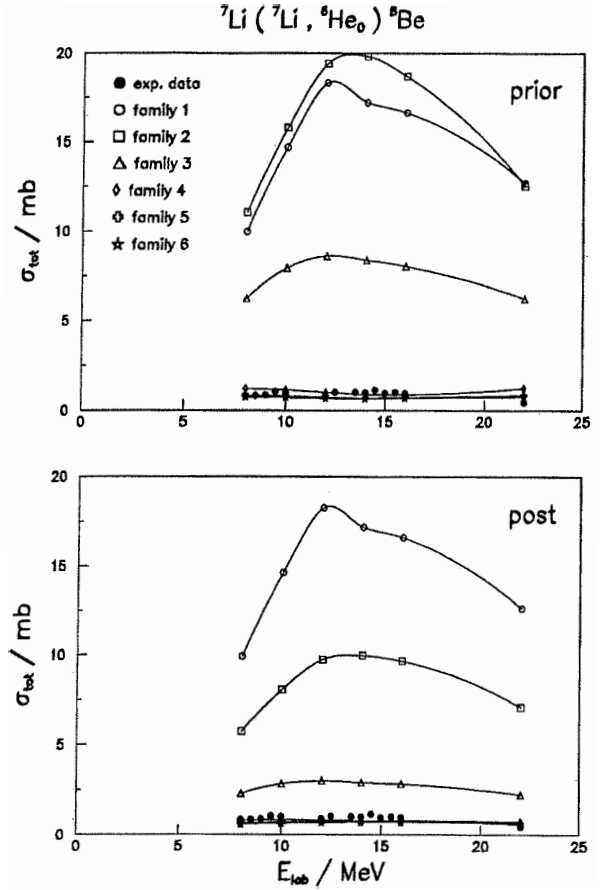


Figure 9: Experimental angle integrated cross sections for the ${}^7\text{Li}({}^7\text{Li}, {}^6\text{He}){}^8\text{Be}_{g.s.}(0^+)$ reaction as a function of projectile energy (solid dots) and results of DWBA calculations performed in *prior* (upper part of the figure) and in *post* representations (lower part). Different lines correspond to the use of different OM potentials (ref. [4]) for the entrance channel and the same OM potential (family #1, i.e. "3 MeV" of [4]) for the exit channel.

calculated with different OM potentials for the entrance ${}^7\text{Li}+{}^7\text{Li}$ channel and with the same,

shallow potential ("3 MeV" family) in the exit channel.

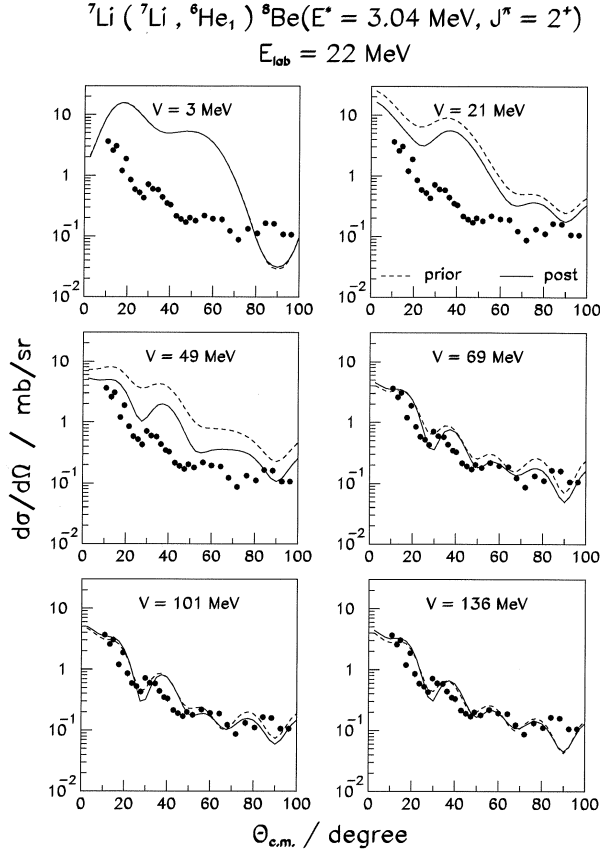


Figure 10: Experimental angular distribution for the ${}^7\text{Li}({}^7\text{Li}, {}^6\text{He}){}^8\text{Be}_{3.04}$ reaction at 22 MeV (lab.) [14] (full dots) and results of DWBA calculations performed with a very shallow (family #1, i.e. "3 MeV" of ref. [4]) ${}^6\text{He}$ - ${}^8\text{Be}$ OM potential and with various ${}^7\text{Li}$ - ${}^7\text{Li}$ OM potentials taken also from ref. [4].

The analysis of the reaction leading to the first excited state of ${}^8\text{Be}$ may yield an additional test of the proton transfer mechanism. In our experiment we were not able to evaluate properly the differential cross sections from the experimental spectra but there are data available of Bochkarev et al. [14] measured for the ${}^7\text{Li}({}^7\text{Li}, {}^6\text{He}){}^8\text{Be}_{3.04}$ reaction at 22 MeV (lab.). Calculations were performed along the

lines which yielded the results shown in Figs. 5 - 8. A very similar picture arises. Therefore we present in Fig. 10 only results of calculations obtained with very shallow ${}^6\text{He}$ - ${}^8\text{Be}$ OM potential ("3 MeV" family) and with various ${}^7\text{Li}$ - ${}^7\text{Li}$ OM potentials. Again only rather deep entrance channel potentials can well describe the experimental data and the quality of this description is quite satisfactory.

From these results we conclude the direct proton transfer to dominate in ${}^7\text{Li}({}^7\text{Li}, {}^6\text{He}){}^8\text{Be}$ reactions and the distorted wave Born approximation to be able to properly describe experimental cross sections in the studied range of energies. The somewhat poorer reproduction of 22 MeV angular distributions may indicate a need for some energy dependence of the optical model potentials (which were fitted to elastic scattering data independently of energy in a restricted range of ${}^7\text{Li}$ projectile energies i.e. 8 - 17 MeV in the lab. system [4]).

3.2 The alpha particle transfer reaction - ${}^7\text{Li}({}^7\text{Li}, t){}^{11}\text{B}$

This reaction seems to be less suited for DWBA in comparison with the proton transfer reaction since the rearrangement of nucleons during alpha particle transfer is more drastic than in proton transfer. Thus it is not clear whether it is appropriate to treat alpha particle transfer in such a light nuclear system as a perturbation. Furthermore, cross sections of alpha particle transfer are typically larger by an order of magnitude than those for proton transfer as can be seen in the Fig.3. They represent approximately 10% of the elastic scattering cross section, a fact which may disqualify the perturbation approach.

The DWBA analysis of the alpha particle transfer was performed along the same lines delineated for proton transfer. Again, no free parameters were allowed for optical model potentials, spectroscopic amplitudes and transition potentials. It was found that results of the calculations are only weakly sensitive to the exit channel $t+{}^{11}\text{B}$ optical model potential. Thus,

in the systematic calculations only one OM potential, taken from the literature (ref. [21]), was used for generating distorted waves in the exit channel.

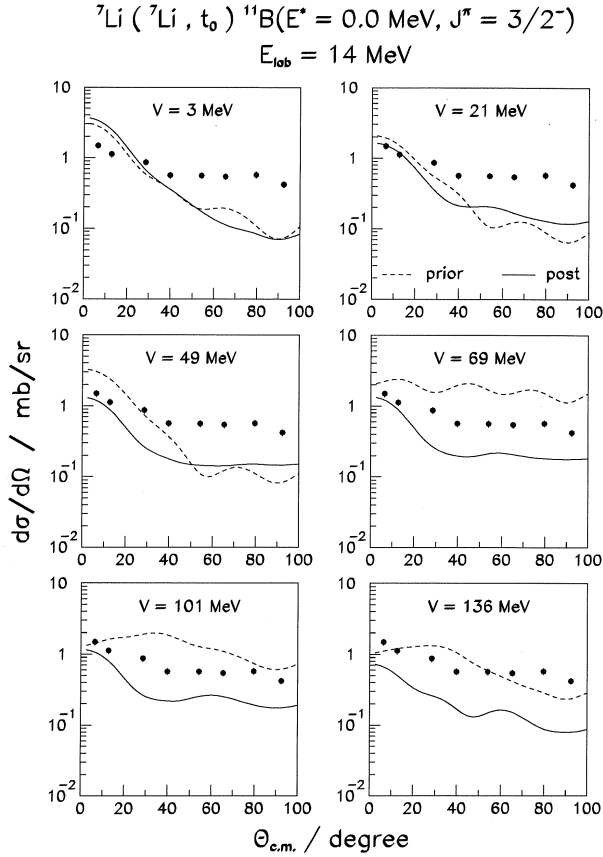


Figure 11: Experimental angular distribution for the ${}^7\text{Li}({}^7\text{Li}, t) {}^{11}\text{B}_{g.s.}(3/2^-)$ reaction at 14 MeV projectile energy (solid dots), and the results of DWBA calculations performed in *prior* (dashed lines) and in *post* representation (full lines). Different frames in the figure correspond to calculations performed with the same ${}^{11}\text{B}$ - t OM potential (ref. [21]) but with different ${}^7\text{Li}$ - ${}^7\text{Li}$ OM potentials of ref. [4]. The depth of the real part of these potentials is given in the corresponding frames.

However, it was found that optical model potentials of the entrance channel which equally well reproduce elastic scattering produce quite

different results when applied in the DWBA. Hence, for comparison, the calculations were performed with the same six OM potentials of the ${}^7\text{Li}+{}^7\text{Li}$ channel which were already used in the analysis of the proton transfer reaction.

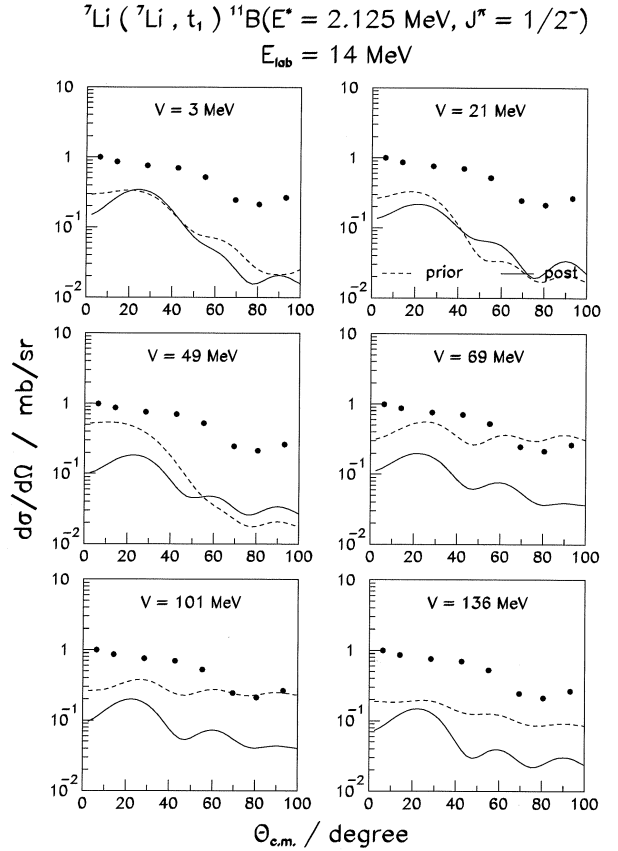


Figure 12: Same as Fig. 11, but for the ${}^7\text{Li}({}^7\text{Li}, t) {}^{11}\text{B}_{2.13}(1/2^-)$ reaction at $E_{\text{lab}}=14$ MeV.

One may conjecture by inspecting Fig. 3 that contributions of mechanisms which are characterized by a strong energy dependence of their cross section e.g. statistical fluctuations and/or excitation of individual resonances, are present in this reaction but least important at the highest energy. Therefore we need to compare both angular distributions and excitation functions as given by DWBA with experimental data.

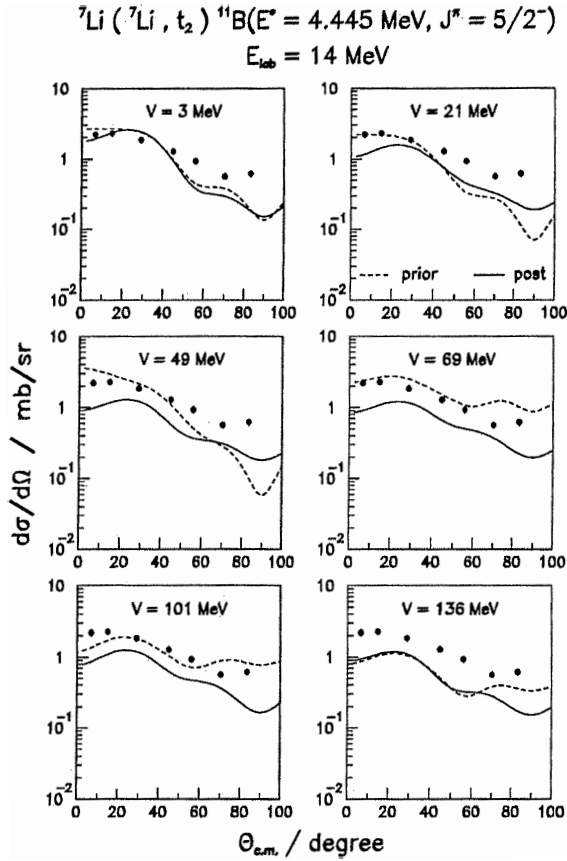


Figure 13: Same as Fig. 11, but for the ${}^7\text{Li}({}^7\text{Li}, t_2){}^{11}\text{B}_{4.45}(5/2^-)$ reaction at $E_{lab}=14$ MeV.

Results of the calculations performed at $E_{lab}=14$ MeV are presented in Fig. 11 for the ground state transfer ${}^7\text{Li}({}^7\text{Li}, t){}^{11}\text{B}_{g.s.}$ and in Figs. 12, 13 and 14 for the transfer to the first (2.13 MeV; $1/2^-$), second (4.45 MeV; $5/2^-$), and third (5.02 MeV; $3/2^-$) excited state, respectively.

The description of the experimental angular distributions by DWBA is acceptable but significantly poorer than for proton transfer. Furthermore, the prior - post equivalence is not well established (especially for deep OM potentials) pointing at the limits of accuracy of the DWBA approach for alpha particle transfer in the ${}^7\text{Li}+{}^7\text{Li}$ system.

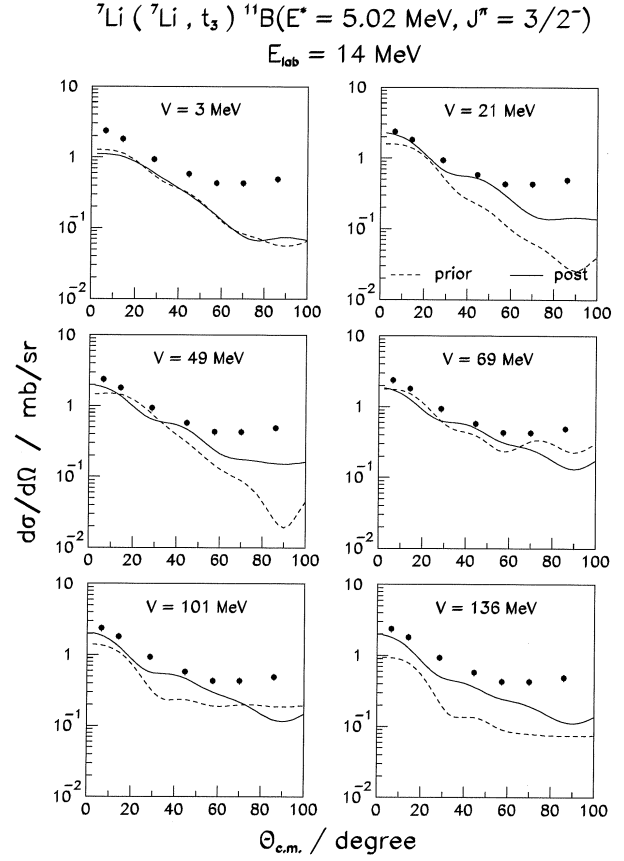


Figure 14: Same as Fig. 11, but for the ${}^7\text{Li}({}^7\text{Li}, t_3){}^{11}\text{B}_{5.02}(3/2^-)$ reaction at $E_{lab}=14$ MeV.

In Figs. 15 - 18 the angle integrated cross sections are depicted versus beam energy. Black dots represent experimental cross sections and the lines correspond to DWBA calculations performed with different ${}^7\text{Li}-{}^7\text{Li}$ OM potentials (cf. Table 1) in *prior* (upper part of the figure) and *post* (lower part of the figure) representations. It may be concluded that results obtained in *post* representation are in general more consistent than those in the *prior* one, i.e. the angle integrated cross sections for all OM potentials yield similar values.

Moreover, the "post - prior" equivalence which was reasonably well fulfilled at $E_{lab}=14$ MeV for shallow potentials remains to be ful-

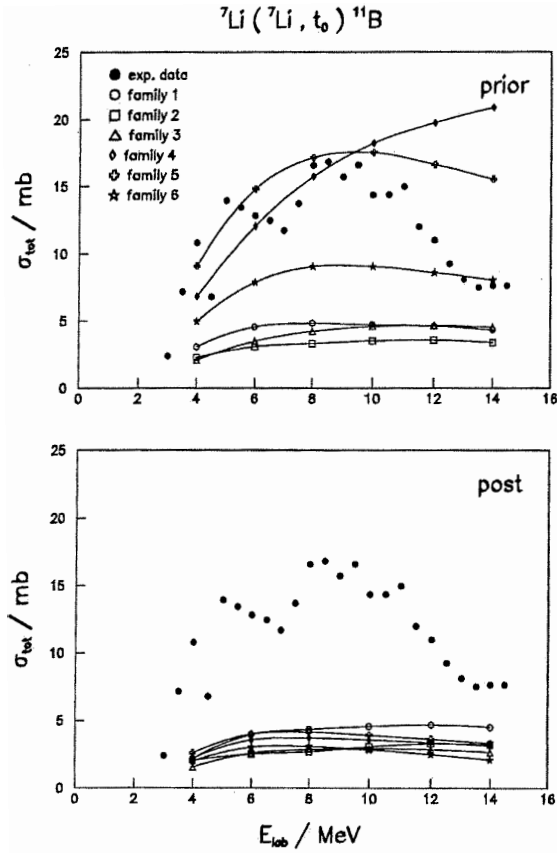


Figure 15: Experimental angle integrated cross section for the ${}^7\text{Li}({}^7\text{Li}, t){}^{11}\text{B}_{g.s.}(3/2^-)$ reaction as a function of projectile energy (solid dots) and results of DWBA calculations performed in *prior* (upper part of the figure) and in *post* representations (lower part). Different lines correspond to the use of different OM potentials for the entrance channel from ref. [4] and the same OM potential (ref. [21]) for the exit channel.

filled for these potentials in the whole energy range. Thus, one has either to use the *post* representation or to choose the shallow potentials for calculations in the *prior* representation. In these cases the shape of the energy dependence of experimental cross sections is reasonably well reproduced by DWBA calculations at least for higher energies. The size of the cross section, however, is predicted too small, clearly show-

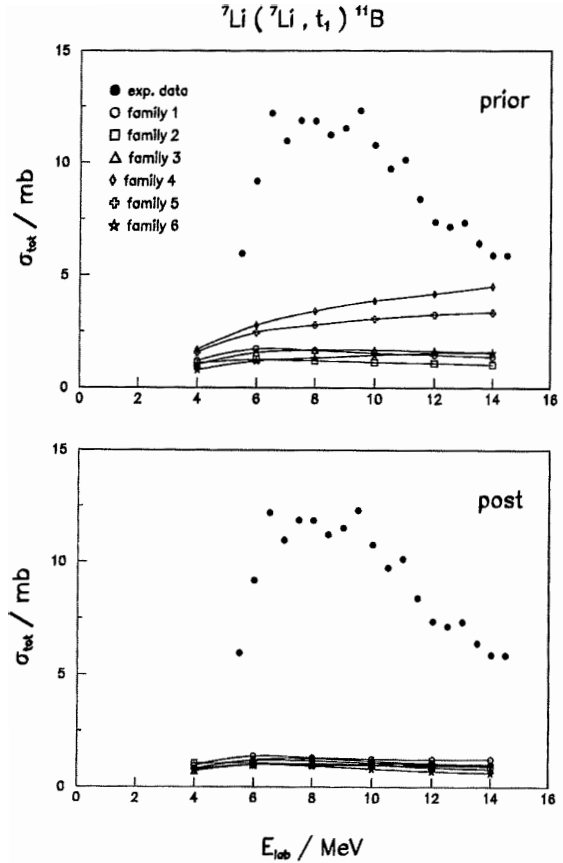


Figure 16: Same as Fig. 15, but for the ${}^7\text{Li}({}^7\text{Li}, t){}^{11}\text{B}_{2.13}(1/2^-)$ reaction.

ing the presence of other reaction mechanisms. DWBA gives an almost constant value of the angle integrated cross section for the ground state transition while the experimental one varies very strongly with energy and has a maximum about $E_{lab} = 8$ MeV.

Resonances are likely to contribute to the triton channel in the low energy region. They exhaust the major part of the experimental cross section. Only at the highest energy of $E_{lab} = 14$ MeV direct reactions become important with contributions of approximately 50% for the ground state transition, and 20%, 50% and 60% for the transitions leading to the first, the second and the third excited states of ${}^{11}\text{B}$, respectively.

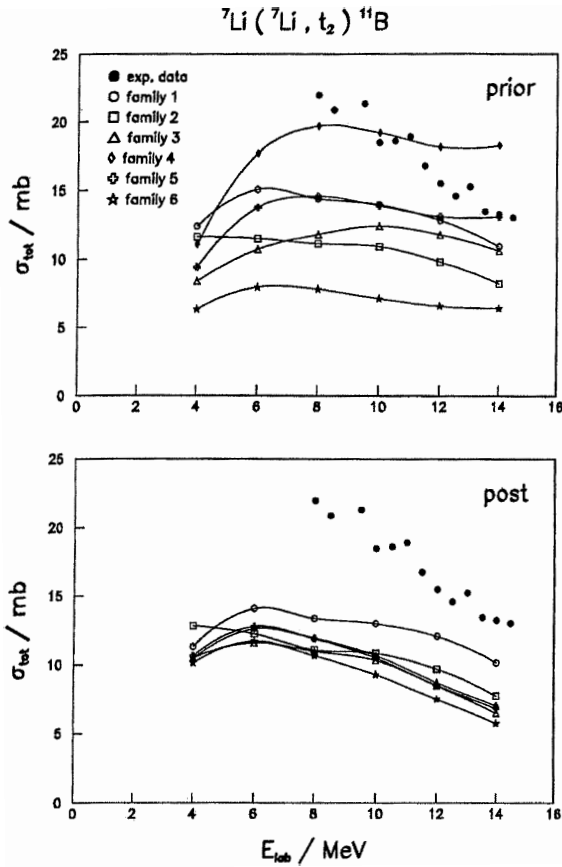


Figure 17: Same as Fig. 15, but for the ${}^7\text{Li}({}^7\text{Li}, t){}^{11}\text{B}_{4.45}(5/2^-)$ reaction.

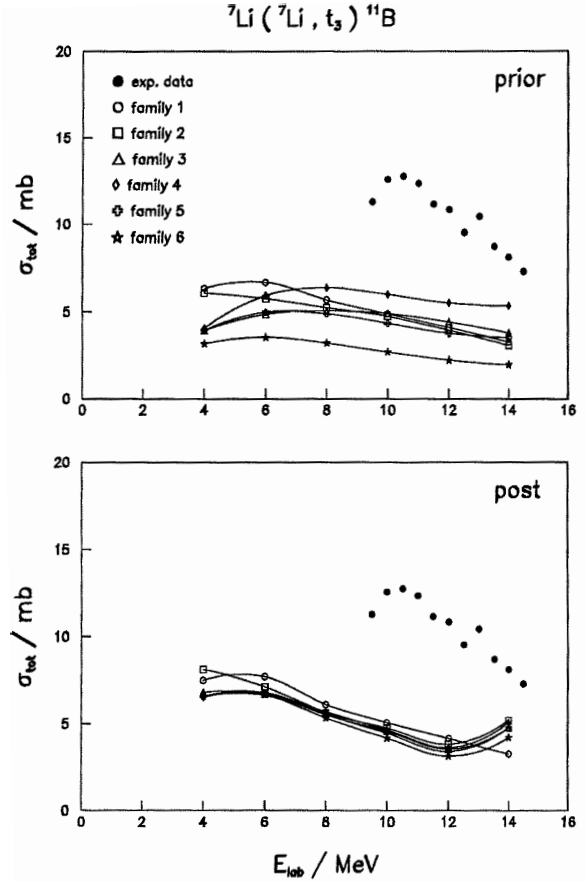


Figure 18: Same as Fig. 15, but for the ${}^7\text{Li}({}^7\text{Li}, t){}^{11}\text{B}_{5.02}(3/2^-)$ reaction.

3.3 The triton transfer reaction - ${}^7\text{Li}({}^7\text{Li}, {}^4\text{He}){}^{10}\text{Be}$

It is apparent from examining Figs. 3 and 4 that a strong variation of the experimental angle integrated cross sections versus energy is present for the ${}^7\text{Li}({}^7\text{Li}, {}^4\text{He})$ reactions. Therefore this channel is the least suited among all reactions under investigation for the application of the direct reaction formalism. Led by results for the alpha particle transfer reactions we can expect DWBA to be appropriate at the highest energy ($E_{\text{lab}}=14$ MeV). DWBA calculations were performed at this energy for transitions to both the ground state of ${}^{10}\text{Be}$ and the first excited state ${}^{10}\text{Be}_{3.37}(2^+)$.

It turned out that in these cases the results of DWBA calculations depend only weakly on the parameters of the exit channel (${}^4\text{He}+{}^{10}\text{Be}$) optical model potential. Hence, only one OM potential was applied for evaluation of distorted waves in the exit channel [20]. All six OM potentials (cf. Table 1) used previously in the analysis of the proton and the alpha particle transfer were exploited for generation of distorted waves in the entrance channel.

The experimental angular distributions (full dots) are shown in Figs. 19 and 20 together with results of DWBA calculations performed using the *prior* (dashed lines) and the *post* representation (full lines) for ${}^7\text{Li}({}^7\text{Li}, {}^4\text{He}){}^{10}\text{Be}_{g.s.}(0^+)$

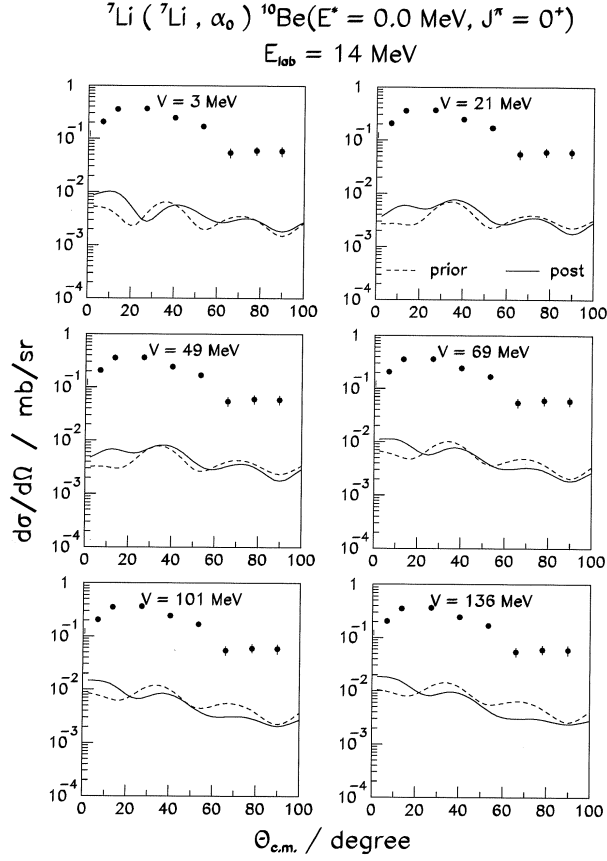


Figure 19: Experimental angular distribution for the ${}^7\text{Li}({}^7\text{Li}, {}^4\text{He}){}^{10}\text{Be}_{g.s.}(0^+)$ reaction at $E_{lab}=14 \text{ MeV}$ (solid dots) and the results of DWBA calculations performed in *prior* (dashed lines) and in *post* representation (full lines). Different frames in the figure correspond to calculations performed with the same ${}^{10}\text{Be}$ - ${}^4\text{He}$ OM potential (ref. [20]) but with different ${}^7\text{Li}$ - ${}^7\text{Li}$ OM potentials from ref. [4]. The depth of the real part of these potentials is given in the corresponding frames.

and ${}^7\text{Li}({}^7\text{Li}, {}^4\text{He}){}^{10}\text{Be}_{3.37}(2^+)$ reactions, respectively. The calculations in both *prior* and *post* representation result in angular distributions similar in shape as well as in magnitude. DWBA angular distributions are in either case smooth with small oscillations reproducing qualitatively the shape of the experimental angular distribu-

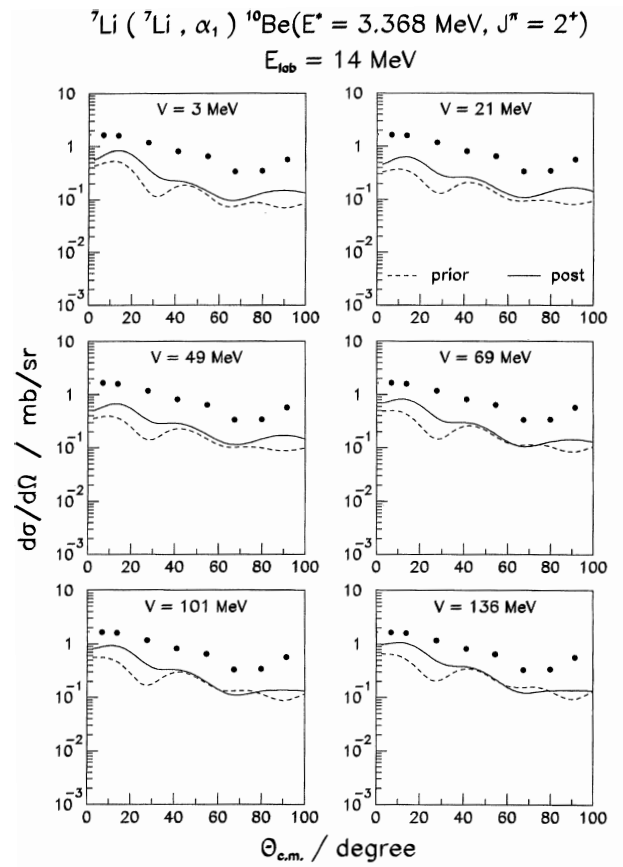


Figure 20: Same as Fig. 19, but for the ${}^7\text{Li}({}^7\text{Li}, {}^4\text{He}){}^{10}\text{Be}_{3.37}(2^+)$ reaction at $E_{lab}=14 \text{ MeV}$.

tions. The magnitude of the theoretical cross sections is, however, in either case smaller than that for the experimental data. In case of the ground state transition the theoretical cross section is smaller by a factor 40 - 50 than the experimental cross section and for alpha transfer leading to the first excited state of ${}^{10}\text{Be}$ the DWBA cross section exhausts approximately 40 - 50 % of the experimental data.

To estimate the average contribution of a direct mechanism to triton transfer the energy dependence of the angle integrated DWBA cross section was calculated and compared with the energy dependence of the experimental angle integrated cross section.

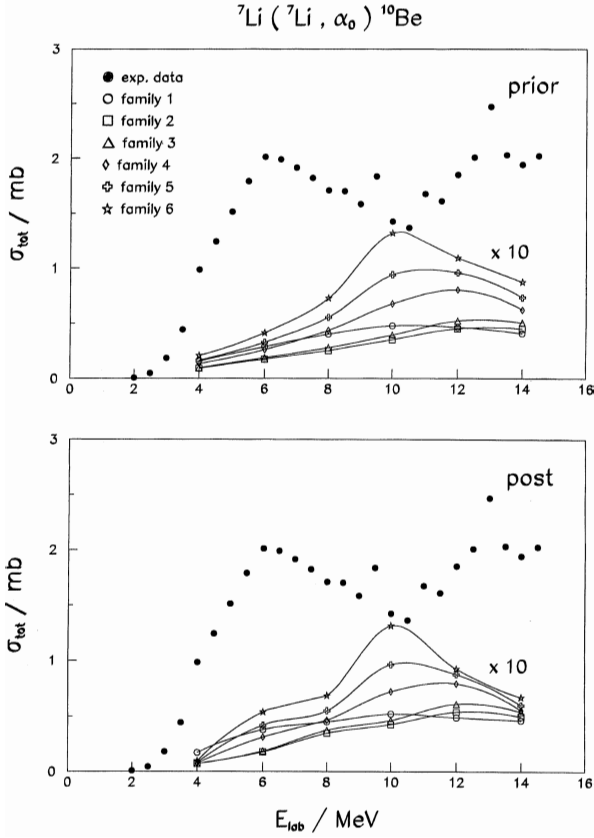


Figure 21: Experimental, angle integrated cross sections for the ${}^7\text{Li}({}^7\text{Li}, {}^4\text{He}){}^{10}\text{Be}_{g.s.}(0^+)$ reaction as a function of projectile energy (solid dots), and results of DWBA calculations performed in *prior* (upper part of the figure) and in *post* representation (lower part). Different lines correspond to the use of different OM potentials (ref. [4]) for the entrance channel and the same OM potential ([20]) for the exit channel.

This is illustrated by Figs. 21 and 22 for the ground state transition and for the transition to the first excited state of ${}^{10}\text{Be}$, respectively. The theoretical cross section for the ground state transition varies smoothly versus energy in the investigated energy range. It is, on average, smaller by a factor 20 - 40 than the experimental cross section. Note that the theoretical cross section shown in Fig. 21 is multiplied by a factor

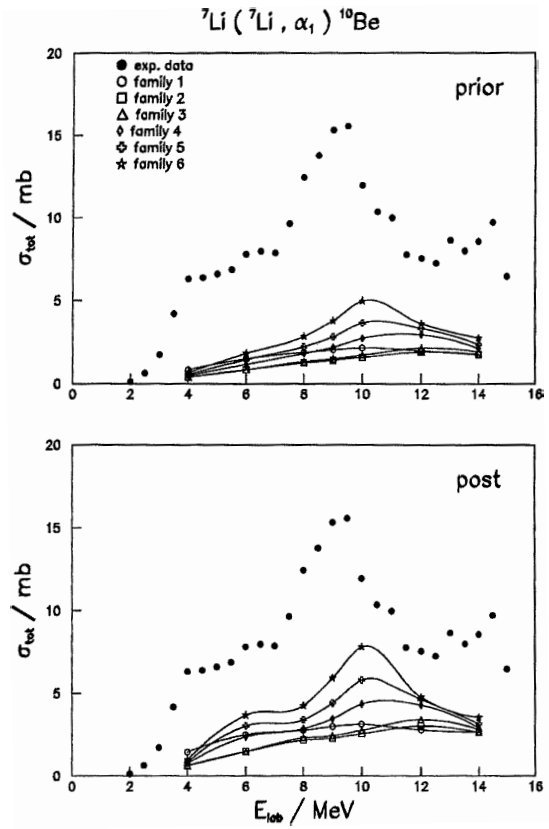


Figure 22: Same as Fig. 21, but for the ${}^7\text{Li}({}^7\text{Li}, {}^4\text{He}){}^{10}\text{Be}_{3.37}(2^+)$ reaction.

of 10 for better representation. In contradistinction to the DWBA predictions the experimental data vary rapidly with energy (the experimental uncertainties are smaller than the dot size in the figure). This is also true for the transition to the first excited state shown in Fig. 22. In this case, however, the theoretical cross section establishes approximately 40 - 50 % of the experimental cross section.

It is interesting to note that the remaining parts of the experimental cross sections which cannot be ascribed to a direct reaction mechanism fulfill a simple " $2J + 1$ " relationship for transitions to both the ground and the first excited state. Such a relationship is indicative for the compound nucleus mechanism. The strong energy dependence of the cross sections seems to

confirm this conjecture.

4 Summary and conclusions

In the present work experimental data are presented from a measurement of angular distributions of ${}^7\text{Li}({}^7\text{Li},\text{t}){}^{11}\text{B}$, ${}^7\text{Li}({}^7\text{Li},{}^4\text{He}){}^{10}\text{Be}$ and ${}^7\text{Li}({}^7\text{Li},{}^6\text{He}){}^8\text{Be}$ reactions at several energies between 8 and 16 MeV in the laboratory system. Transitions to the ground states as well as to some low lying excited states (three in the triton channel and one in the ${}^4\text{He}$ channel) were studied. Already by inspection of these data we are led to the conclusion that the $({}^7\text{Li},{}^6\text{He})$ reaction proceeds predominantly as a direct process while various mechanisms may contribute to $({}^7\text{Li},\text{t})$ and $({}^7\text{Li},\alpha)$ reactions. The latter reaction seems to proceed predominantly through isolated resonances of the ${}^{14}\text{C}$ compound system.

A DWBA analysis was performed for all channels, the results confirm the qualitative conclusions derived from inspection of the experimental data. The $({}^7\text{Li},{}^6\text{He})$ reaction is - within the accuracy of DWBA calculations - completely described by direct proton transfer. The other two reactions proceed partially by direct mechanisms: in average 20 - 60 % for the α -particle transfers $({}^7\text{Li},\text{t})$ and 40 - 50 % for the triton transfer $({}^7\text{Li},{}^4\text{He})$ reaction to the first excited state of ${}^{10}\text{Be}$ and only approximately 3 - 5 % for transition to the ground state.

Estimations based on the Hauser-Feshbach model [5] indicate a rather small contribution of compound nucleus reactions (approximately 12-20% for the triton channels and even less for α particle and ${}^6\text{He}$ channels). Thus, processes different than pure direct and pure compound nucleus mechanisms are present in the investigated energy range. The interference between direct and compound nucleus reaction - amplitudes may lead to fluctuations of the cross section which, however, are expected to be narrower (typical width approx. 0.6 MeV) than the structures observed here. Indeed, the presence of

strong peaks in the excitation functions of the angle integrated cross section for α_1 , correlated with the structures visible in the excitation function measured at forward angles suggests a contribution of isolated resonances superimposed on the background from both direct and statistical compound nucleus reactions.

The good reproduction of both shape and magnitude of the experimental angular distributions for the ${}^7\text{Li}({}^7\text{Li},{}^6\text{He}){}^8\text{Be}$ reaction by the DWBA calculations as well as the reproduction of the energy dependence of the cross section indicates that the methods of direct reaction theory can be successfully applied for such a system of few nucleons. The calculations within both *prior* and *post* representations lead to equivalent results and thus manifest the adequacy of the DWBA approach to this reaction. The use of different optical model potentials in the DWBA calculations allowed us to select from potentials which describe elastic and inelastic scattering equally well those which are appropriate, namely a rather deep (appr. 70 MeV) OM potential for the entrance $({}^7\text{Li}+{}^7\text{Li})$ and a very shallow potential (approx. 3 MeV) for the exit $({}^6\text{He}+{}^8\text{Be})$ channel. Only this combination of OM potentials produces results which agree with the experimental data of the ${}^7\text{Li}({}^7\text{Li},{}^6\text{He}){}^8\text{Be}$ reaction.

In spite of rather big cross sections for the α particle and triton channels (approximately 10% of the elastic cross section) and the relatively strong rearrangement processes of the ${}^7\text{Li}+{}^7\text{Li}$ system after triton or α particle transfer the method of DWBA can be successfully applied to evaluate the contribution of the direct mechanism to the ${}^7\text{Li}({}^7\text{Li},{}^4\text{He}){}^{10}\text{Be}$ and ${}^7\text{Li}({}^7\text{Li},\text{t}){}^{11}\text{B}$ reactions. Results of DWBA calculations turned out to be insensitive to variation of the exit channel optical model potentials in both cases but some caution is in order when applying the *prior* or *post* representations together with different OM potentials in the entrance channel. In general the *post* representation is superior and may be applied without further selection of the optical model potentials. The calculations in the *prior* repre-

sentation lead to equivalent results, as it is demanded by the DWBA formalism, only if optical model potentials of the ${}^7\text{Li}+{}^7\text{Li}$ system are chosen which are rather shallow (< 60 MeV). A selection of ${}^7\text{Li}+{}^7\text{Li}$ OM potentials on the basis of DWBA calculations applied to triton and α particle transfers yields results contrary to those obtained for the proton transfer. This may indicate that either the proton transfer reaction is sensitive to different parts of the OM potential than the cluster transfers or the *prior* representation is not well suited for these reactions e.g. due to poor cancellation of "indirect transition" potentials.

It should be emphasized that the good description of the experimental data by DWBA was achieved without introducing any free parameters. This strongly supports the applicability of DWBA for the ${}^7\text{Li}+{}^7\text{Li}$ system although, at first sight, the methods of direct reaction theory seem hardly adequate for a system consisting of such a small number of nucleons.

Acknowledgements: We are grateful to Dr. E. Kwaśniewicz for supplying spectroscopic amplitudes.

References

- [1] Domogala, G., Freiesleben, H., Nucl. Phys. **A467**, 149 (1987)
- [2] Wiebach, S., Bachmann, A.M., Brand, H., Eule, R.P., Freiesleben, H., Heyber B., Leifels, Y., Potthast, K.W., Rosenthal, P., Kamys, B., Z. Phys. **A346**, 173 (1993)
- [3] Leifels, Y., Domogala, G., Eule, R.P., Freiesleben, H., Z. Phys. **A335**, 183 (1990)
- [4] Bachmann, A.M., Brand, H., Freiesleben, H., Leifels, Y., Potthast, K.W., Rosenthal, P., Kamys, B., Z. Phys. **A346**, 47 (1993)
- [5] Gotzhein, I., Diploma thesis, Bochum 1989 - unpublished
- [6] Huberman, M.N., Kamegai, M., Morrison, G.C., Phys. Rev. **129**, 791 (1963)
- [7] Dzubay, T.G., Blair, J.M., Phys. Rev. **B134**, 586 (1964)
- [8] Carlson, R.R., Wyborny, H.W., Phys. Rev. **178**, 1529 (1968)
- [9] Wyborny, H.W., Carlson, R.R., Phys. Rev. **C3**, 2185 (1971)
- [10] Glukhov, Y.A., Novatskii, B.G., Ogloblin, A.A., Sakuta, S.B., Stepanov, D.N., Chuev, V.I., Sov. J. Nucl. Phys. **13**, 154 (1971); (Yad. Fiz. **13**, 277 (1971))
- [11] Cerny, J., Weisenmiller, R.B., Jelley, N.A., Wilcox, K.H., Wozniak, G.J., Phys. Lett. **53B**, 247 (1974)
- [12] Carlson, R.R., McGrath, R.L., Norbeck, E., Phys. Rev. **B136**, 1687 (1964)
- [13] Stryk, R.A., Blair, J.M., Phys. Rev. **169**, 767 (1968)
- [14] Bochkarev, O.V., Korshennikov, A.A., Kuźmin, E.A., Mukha, I.G., Chulkov, L.V., Yańkov, G.B., Sov. J. Nucl. Phys. **47**, 391 (1988) (Yad. Fiz. **47**, 616 (1988))
- [15] Domogala, G., Freiesleben, H., Hippert, B., Nucl. Instr. Meth. in Phys. Research **A257**, 1 (1987)
- [16] Tamura, T., Udagawa, T., Mermaz, M.C., Phys. Rep. **65**, 345 (1980); Program Jupiter-5, modified by Kamys, B., Rudy, Z., Wolter, H.H., Zittel W., to allow for particles with non-zero spin in the entrance channel
- [17] Satchler, G.R., Direct Nuclear Reactions, Clarendon Press, Oxford 1983
- [18] Oelert, W., Djoelis, A., Mayer-Boericke, C., Turek, P., Phys. Rev. **C19**, 1747 (1979)
- [19] Kamys, B., Rudy, Z., - SQSYM computer program, 1988 - unpublished

- [20] England, J.B.A., Casal, E., Garcia, A., Picazo, T., Aguilar, J., Sen Gupta, H.M., Nuclear Physics **A284**, 29 (1977)
- [21] Harakeh, M.N., Van Popta, J., Saha, A., Siemssen, R.H., Nucl. Phys. **A344**, 15 (1980)
- [22] Kwaśniewicz, E., Kisiel, J., J. of Phys. **G13**, 121 (1987)
- [23] Kurath, D., Millener, D.J., Nucl. Phys. **A238**, 269 (1975)
- [24] Kwaśniewicz, E., private information (1989)
- [25] Kurath, D., Phys. Rev. **C7**, 1390 (1973)
- [26] Kwaśniewicz, E., Jarczyk, L., J. of Phys. **G12**, 697 (1986)
- [27] Kwaśniewicz, E., private information (1986)